CV-QKD Receiver Platform Based On A Silicon Photonic Integrated Circuit

Yoann Piétri,[1,*] Luis Trigo Vidarte,[2] Matteo Schiavon,[1] Philippe Grangier,[3] Amine Rhouni,[1] and Eleni Diamanti[1]

[1] *Sorbonne Université, CNRS, LIP6, F-75005 Paris, France*
[2] *ICFO - Institut de Ciències Fotòniques, The Barcelona Institute of Science and Technology, Castelldefels (Barcelona) 08860, Spain*
[3] *Université Paris-Saclay, Institut d'Optique Graduate School, CNRS, Laboratoire Charles Fabry, 91127, Palaiseau, France*
[*] *Yoann.Pietri@lip6.fr*

Abstract: We report on the characterization of a SiGe PIC-based receiver along with its usage in a Gaussian-modulated coherent state CV-QKD setup. Excess noise measurements lead to secret key rate estimations of 280 kbit/s at 6.9 km.

1. Introduction

Quantum Key Distribution (QKD) is a prominent application of quantum cryptography and it allows two trusted users, usually referred to as Alice and Bob, to exchange a cryptographic secret key with a security based on the laws of physics. This means that any eavesdropper bounded only by physical laws will have no meaningful information on the exchanged key.

In widely-used Discrete-Variable QKD (DV-QKD), information is encoded on discrete degrees of freedom such as the polarization of single photons and their implementation requires dedicated technology such as single-photon detectors. Conversely, in Continuous-Variable QKD (CV-QKD) information is encoded on continuous degrees of freedom such as the quadratures of the electromagnetic field making their implementation compatible with standard telecom components and infrastructures, and thus reducing the overall complexity and cost of QKD [1]. Recent works also suggest that CV-QKD allows for record high secret key rates at moderate distances [2].

In order to reduce the cost and size of QKD systems even more and to facilitate the deployment of QKD in practical infrastructures, significant efforts have been made towards integrating those systems on Photonic Integrated Circuits (PICs) [3]. While integration is a challenge for both DV-QKD and CV-QKD, CV-QKD doesn't require the integration of cryogenic single-photon detectors and is, in principle, more straightforward and less costly as only standard, room temperature components are required [4].

In this work, we present a Si integrated receiver platform for Gaussian-modulated coherent state CV-QKD with Optical Single Side Band Modulation (GMCS-OSSB).

2. Description of the CV-QKD receiver platform

The receiver platform is composed of two parts: the photonic chip and the electronic circuit for amplification. The photonic chip was fabricated by LETI-CEA using a SiGe process and its layout is given in Fig. 1. The chip is composed of two 180° hybrid balanced detectors. Each detector includes two grating couplers that are the inputs and going into a 50:50 beam splitter. Each output arm of the beam splitter goes through wave guides into an electrically driven Variable Optical Attenuator (VOA) that is used to perfectly balance the detection, which is critical for the application. Finally the outputs of the VOAs go into the two photodiodes.

The photonic chip is wirebonded to the Printed Circuit Board (PCB), to reduce the parasitic capacitances and hence increase the bandwidth of the receiver. The PCB was designed in our laboratory, with commercially available components to reach ultra-low electronic noise and shot-noise limited receiver. The balanced detector amplification chain is composed of a TIA (Trans-Impedance Amplifier) and a V/V amplifier.

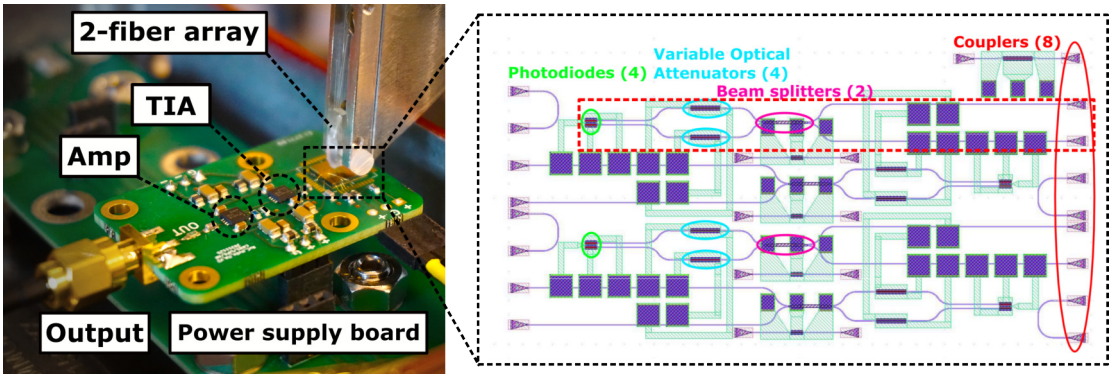

Fig. 1: Layout and picture of the chip and receiver. On the left, picture of the receiver in the setup. The receiver card is plugged on a power supply board. A fiber array on a three axis stage allows for light coupling. We can see on the card a Trans-Impedance Amplifier and a V/V amplifier. On the right, layout of the photonic chip.

3. Experimental results and expected performance for CV-QKD

The receiver was first characterized as a standalone device, to verify its linearity, its efficiency and its clearance (shot-noise-to-electronic-noise ratio), which are all critical parameters for CV-QKD. We report a 26% maximal receiver detection efficiency, a linearity of 99.2% up to 8 mW of local oscillator power and a clearance of more than 20 dB at low frequencies and more than 7 dB for 250 MHz.

We then included the receiver in our CV-QKD setup. The transmitter side, Alice, is composed of bulk components including a continuous wave laser, an IQ modulator, a bias controller, a monitoring photodiode and attenuators. The signal is sent to the receiver, Bob, through a polarization-maintaining VOA that is used to emulate channel attenuation. The continuous wave laser is split and transmitted into a different fiber to be used as a local oscillator. The experimental scheme is shown in Fig. 2.

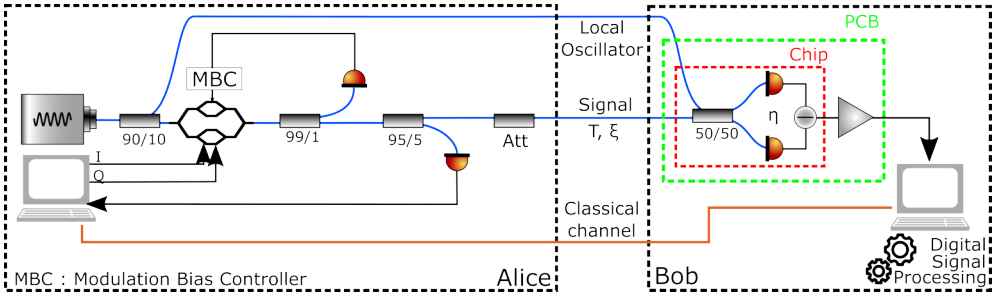

Fig. 2: Experimental Scheme. Alice is composed of a continuous wave laser splitted for signal generation and transmitted local oscillator. On the signal generation path, light goes through an IQ modulator, driven by an Arbitrary Waveform Generator, a modulation bias controller, a monitoring photodiode and a variable optical attenuator. On Bob's side, the signal is mixed with the transmitted local oscillator and detected on the chip. The output is amplified and acquired by an Analog-To-Digital converter. Important parameters are the mean number of photons on Alice's side $\langle n \rangle = \frac{V_A}{2}$ that is measured using the second photodiode, T the transmittance of the channel, ξ the excess noise of the channel as seen at the channel input, V_{el} the electronic noise of the detector, η the efficiency of the detector and β the efficiency of the reconciliation process.

The exchanged data at 100MBaud (100MSymbols/s) was processed using a specifically designed and fine-tuned Digital Signal Processing (DSP) algorithm. DSP on Alice's side includes symbol generation, pulse shaping, frequency shift, and phase reference pilots, and on Bob's side synchronization, clock recovery, match filtering, best sampling point finding and relative and global phase correction.

We then proceeded to parameter estimation for the excess noise, the attenuation and Alice's modulation strength using the covariance matrix estimation method [5, 6], which allows us to estimate the expected secret key rate. An excess noise measurement was performed over 5 hours, which proved that our receiver is stable, and yielded an average value of $\xi = 0.102$ SNU (see Fig. 3(a)). The measurement was performed at a channel attenuation of 1.38 dB, corresponding to an equivalent distance of 6.9 km (at 0.2 dB/km). The expected key rate is plotted in Fig. 3(b) (black line). An expected key rate of 280 kbit/s was found for the attenuation of 1.38 dB.

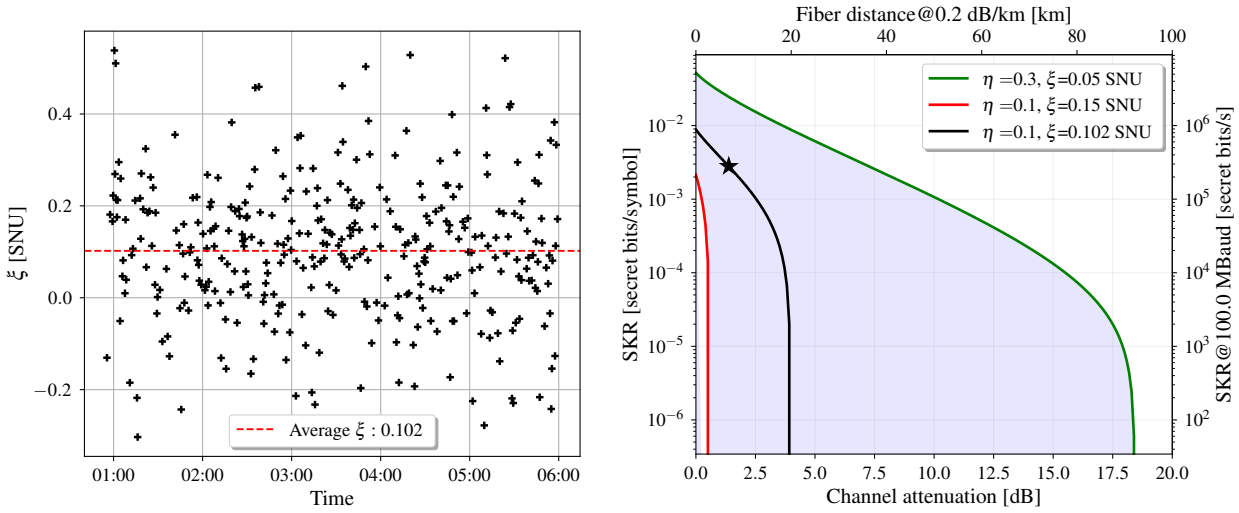

Fig. 3: Expected CV-QKD performance. On the left, plot of the excess noise ξ at Alice's side. The excess noise at Bob ξ_B and the total attenuation ηT are estimated using the covariance matrix method (with V_A estimated on Alice's side). The value of excess noise ξ is then computed with $\xi = \frac{\xi_B}{\eta T}$ and plotted against time. On the right, asymptotic secret key rate estimation under the assumptions of Gaussian modulation and trusted detection. We also show for comparison plots corresponding to different values of η and ξ (red and green lines). Other parameters are $V_A = 1$ SNU, $\beta = 0.95$, Symbol rate: 100 MBaud, $V_{\text{el}} = 0.03$ SNU. Star point is the expected secret key rate at 6.9 km: 280 kbit/s.

4. Conclusion

We presented a coherent receiver platform based on a silicon photonics PIC with promising characteristics for CV-QKD along with excess noise measurements that yield positive secret key rates at metropolitan distances, with an expected key rate of 280 kbit/s at 6.9 km.

Near term future work includes fine-tuning the parameters to reduce further the excess noise, implementing a scheme with a true local oscillator, extracting a key with post-processing algorithms and performing a CV-QKD exchange between a PIC-based emitter and a PIC-based receiver.

Clearance	Linearity	Bandwidth	η	Heterodyne	Balanced	V_A	Excess noise
26 dB @ 10MHz 14dB @ 100 MHz 9dB @ 200MHz 7dB @ 250MHz	99.20%	250 MHz	26%	RF	Yes (VOA)	1 SNU	0.102 SNU

Table 1: Summary of the performances of the PIC-based receiver platform.

References

1. P. Jouguet, S. Kunz-Jacques, A. Leverrier, P. Grangier, E. Diamanti, Experimental demonstration of long-distance continuous-variable quantum key distribution, Nature Photon. 7, 378 (2013).
2. F. Roumestan, A. Ghasizaeidi, J. Rénaudier, L. Trigo Vidarte, E. Diamanti, P. Grangier, High-Rate Continuous Variable Quantum Key Distribution Based on Probabilistically Shaped 64 and 256-QAM, ECOC 2021, arXiv:2111.12356 [quant-ph].
3. G. Zhang *et al.*, An integrated silicon photonic chip platform for continuous-variable quantum key distribution, Nature Photon. 13, 839 (2019).
4. Q. Liu, Y. Huang, Y. Du, Z. Zhao, M. Geng, Z. Zhang, K. Wei, Advances in Chip-Based Quantum Key Distribution, Entropy 24(10), 1334 (2022).
5. S. Fossier, E. Diamanti, T. Debuisschert, R. Tualle-Brouri, P. Grangier, Improvement of continuous-variable quantum key distribution systems by using optical preamplifiers. Journal of Physics B: Atomic, Molecular and Optical Physics 42(11), 114014 (2009).
6. F. Laudenbach, C. Pacher, C. Fred Fung, A. Poppe, M. Peev, B. Schrenk, M. Hentschel, P. Walther, H. Hübel, Continuous-Variable Quantum Key Distribution with Gaussian Modulation-The Theory of Practical Implementations. Advanced Quantum Technologies 1(1), 1800011 (2018).